

# Unusual Growth Behavior of Atomic Layer Deposited PbTiO<sub>3</sub> Thin Films Using Water and Ozone As Oxygen Sources and Their Combination

Hyun Ju Lee,<sup>†</sup> Min Hyuk Park,<sup>†</sup> Yo-Sep Min,<sup>‡</sup> Guylhaine Clavel,<sup>§</sup> Nicola Pinna,<sup>§,||</sup> and Cheol Seong Hwang<sup>\*,†</sup>

WCU Hybrid Materials Program, Department of Materials Science and Engineering and Inter-university Semiconductor Research Center, Seoul National University, Seoul 151-744, Korea, Department of Chemical Engineering, Konkuk University, Seoul 143-701, Korea, Department of Chemistry, CICECO, University of Aveiro, 3810-193 Aveiro, Portugal, and WCU Program of Chemical Convergence for Energy & Environment (C2E2), School of Chemical and Biological Engineering, College of Engineering, Seoul National University, Seoul 151-744, Korea

Received: February 16, 2010; Revised Manuscript Received: June 10, 2010

PbTiO<sub>3</sub> thin films were deposited on Si and Ru substrates by atomic layer deposition at a substrate temperature of 200 °C using H<sub>2</sub>O and O<sub>3</sub> as oxygen sources and lead(II) bis(3-*N,N*-dimethylamino-2-methyl-2-propoxide) and titanium(IV) isopropoxide as the Pb and Ti precursors, respectively. When H<sub>2</sub>O was used as the oxygen source for both Pb and Ti precursors, film growth was most effective under the conditions where a stoichiometric PTO film was achieved (Pb/Ti concentration ratio ~ 1). On the other hand, the PTO growth per cycle increased with increasing the PbO<sub>x</sub>/TiO<sub>2</sub> subcycle ratio when O<sub>3</sub> was used as the oxygen source for the Ti precursor, even when Pb-rich PTO films were deposited. These unexpected results were explained by the different reactions occurring according to the oxygen source used, in particular, by a reaction mechanism involving the direct condensation between surface formate species and alkoxy species in the case of ozone.

## I. Introduction

Atomic layer deposition (ALD) is generally characterized by a unique self-regulated growth behavior owing to its surface saturating growth mechanism.<sup>1</sup> ALD consists of precursor and reactant pulse steps, followed by an inert gas purging step for the precursor/reactant. This cyclic process enables conformal deposition and precise control of both the film thickness and the composition due to its inherent self-limiting growth nature.

However, there are only few reports on the use of ALD for the growth of multimetal ferroelectric oxide thin films, such as Pb(Zr, Ti)O<sub>3</sub> (PZT) and PbTiO<sub>3</sub> (PTO), which have remanent polarization (*P<sub>r</sub>*) even in the absence of an external electric field.<sup>2</sup> This is because ALD processes for multicomponent oxide films are usually quite complicated and achieving the desired stoichiometry is dependent on the chemical reactivity of the precursors and reactants used. In addition, the surface structure during ALD is usually much more complex than that of simpler binary oxides. Recently, Harjuoja et al. fabricated ALD PTO films using tetraphenyl lead [Pb<sub>4</sub>Pb] and titanium(IV) isopropoxide [Ti(O<sup>*i*</sup>Pr)<sub>4</sub>] and obtained a perovskite structure after postdeposition annealing (PDA).<sup>3</sup> Hwang et al. reported ALD of PTO films using lead bis(3-*N,N*-dimethylamino-2-methyl-2-propoxide) [Pb(DMAMP)<sub>2</sub>], titanium tetra(*tert*-butoxide) [Ti(O<sup>*t*</sup>Bu)<sub>4</sub>], and H<sub>2</sub>O at a growth temperature of 200 °C, where an amorphous film was obtained. The films were crystallized by PDA, but in many cases, they also contained the pyrochlore phase along the grain boundaries, which was dependent on the PDA methods.

After proper PDA, the films showed ferroelectric switching behavior but were slightly electrically leaky.<sup>4</sup> Watanabe et al. reported the uniform deposition of stoichiometric PTO films on a 3D structure using ALD.<sup>5</sup> They also fabricated ALD PZT films using bis(dipivaloylmethanato) lead [Pb-(DPM)<sub>2</sub>], Ti(O<sup>*i*</sup>Pr)<sub>4</sub>, and tetrakis(dipivaloylmethanato) zirconium [Zr(DPM)<sub>4</sub>]. However, it was difficult to incorporate Zr into the film. The Zr/(Zr + Ti) ratio in the PZT films was <0.1 despite modifications to the precursor-injection sequence.<sup>6</sup> To solve this problem, they changed the Zr precursor to tetrakis(diisobutylmethanato) zirconium [Zr(DIBM)<sub>4</sub>], and PZT films with a Zr/(Zr + Ti) ratio of >0.2 were obtained. However, the as-deposited PZT film on a 3D structure was a composite of crystallized PbO<sub>x</sub> nanoclusters and amorphous Ti–Zr–O, not a homogeneous PZT phase.<sup>7</sup> These reports highlight the difficulty in multicomponent PZT (and PTO) ALD and the importance of the type of precursor used. ALD is generally more dependent on the types of precursors and reactants than MOCVD, which further complicates the development of ALD processes to a level that can be used in the semiconductor industry.

In addition, the types of oxygen sources, such as H<sub>2</sub>O, O<sub>3</sub>, and O<sub>2</sub> plasma, also have a substantial influence on the surface chemical reaction and resulting growth behavior of oxide films. Only recently, these effects were considered seriously, even for simpler binary oxides, such as HfO<sub>2</sub>.<sup>8,9</sup> In ALD of oxide films, –OH groups play a key role as the anchoring sites for the approaching precursor molecules, which improves the film growth per cycle.<sup>10</sup> The role of O<sub>3</sub> as the oxygen source in ALD of oxide thin films is more controversial even for simpler binary oxides, such as Al<sub>2</sub>O<sub>3</sub> and HfO<sub>2</sub>. For multimetal oxides, such as PTO, the same or different type of oxygen source can be used for each metal precursor, which largely complicates the understanding of the ALD reaction mechanism. Nevertheless,

\* To whom correspondence should be addressed. E-mail: cheolsh@snu.ac.kr.

<sup>†</sup> Department of Materials Science and Engineering and Inter-university Semiconductor Research Center, Seoul National University.

<sup>‡</sup> Konkuk University.

<sup>§</sup> University of Aveiro.

<sup>||</sup> College of Engineering, Seoul National University.

this may be a viable approach for improving the growth behavior and the electrical properties of the films.

In this study, as a prototype of PZT thin films, PTO thin films were deposited on Si and Ru substrates by ALD using different oxygen sources (H<sub>2</sub>O and O<sub>3</sub>) for the Ti precursor and H<sub>2</sub>O as the oxygen source for the Pb precursor. The growth behavior and catalytic effect observed during PTO film ALD were examined. The effect of the oxygen sources on the growth behavior of its component oxide, TiO<sub>2</sub> and PbO<sub>x</sub> thin films, was also investigated to determine the growth behavior of the PTO films using different oxygen sources for the Ti precursor. The electrical properties of the films will be reported elsewhere.

## II. Experimental Procedure

PbO<sub>x</sub>, TiO<sub>2</sub>, and PTO films were grown at a growth temperature of 200 °C using a 4 in. scale traveling-wave type ALD reactor (Quoros Co., Plus 100). Si and Ru(30 nm)/TaO<sub>x</sub>/Si were used as substrates. A Ru electrode was used in this study because the deposition of a Ru film by either MOCVD or ALD has been studied extensively for applications to capacitors in dynamic random access memory.<sup>11–14</sup> Lead bis(3-*N,N*-dimethyl-amino-2-methyl-2-propoxide) [Pb(DMAMP)<sub>2</sub>] and Ti(O<sup>*i*</sup>Pr)<sub>4</sub> were used as the Pb and Ti precursors, respectively. H<sub>2</sub>O and O<sub>3</sub> were used as the oxygen sources, and Ar was used as the purging gas. Pb(DMAMP)<sub>2</sub> and Ti(O<sup>*i*</sup>Pr)<sub>4</sub> were evaporated separately from stainless steel canisters kept at 90 and 65 °C, respectively, in order to ensure adequate vapor pressure of the respective precursors. The precursors were supplied to the reactor using the standard bubbling technique. Ar carrier gas (35 sccm (standard cubic centimeters per minute)) was used for Pb precursor delivery, whereas no carrier gas was used for Ti precursor delivery. H<sub>2</sub>O was evaporated at 3.0 °C and transported to the reactor without a carrier gas. The H<sub>2</sub>O pulse and purging times were 1 and 35 s, respectively. The very long H<sub>2</sub>O purging time was necessary to ensure the ALD reaction due to the inefficient H<sub>2</sub>O purging process at such a low deposition temperature (200 °C). O<sub>3</sub> was produced from an induction-type O<sub>3</sub> generator (Astex, AX8200) at a concentration of ~260 g/m<sup>3</sup> using an O<sub>2</sub>/N<sub>2</sub> gas mixture (N<sub>2</sub> concentration of 0.74%). The O<sub>3</sub> pulse and purging times were 3 and 10 s, respectively. The base pressure of the ALD chamber was 0.04 Torr, and the working pressure during the Ar purging step was ~0.9 Torr. The flow rate of the Ar purging gas was 535 sccm for the Pb precursor and 500 sccm for the Ti precursor, H<sub>2</sub>O and O<sub>3</sub>. The precursor pulse/purging times for the Pb and Ti precursors were determined by the conditions that ensured a self-saturation growth behavior of the component oxides from preliminary experiments. The optimal Pb precursor pulse and purging times were 0.5 and 30 s, respectively, and the optimal Ti precursor pulse and purging times were 3 and 5 s, respectively.

The layer density (LD) was measured by X-ray fluorescence spectroscopy (XRF, Thermo Electron Co., QUANT'X), and the atomic concentrations of Pb and Ti of PTO films were determined. The LD is the total mass over the entire film thickness of Pb (or Ti) atoms that are deposited on the unit area (cm<sup>2</sup>) of the substrate with a unit of μg/cm<sup>2</sup>. The LD (μg/cm<sup>2</sup>) measured by XRF was converted to a value with units of atoms/nm<sup>2</sup> using the atomic masses of Pb and Ti atoms. The LD growth per cycle (GPC) can be achieved by dividing it by the number of growth cycles. The film thickness was measured by ellipsometry. Auger electron spectroscopy (AES, PerkinElmer 660) was used to analyze the composition along the film thickness direction.

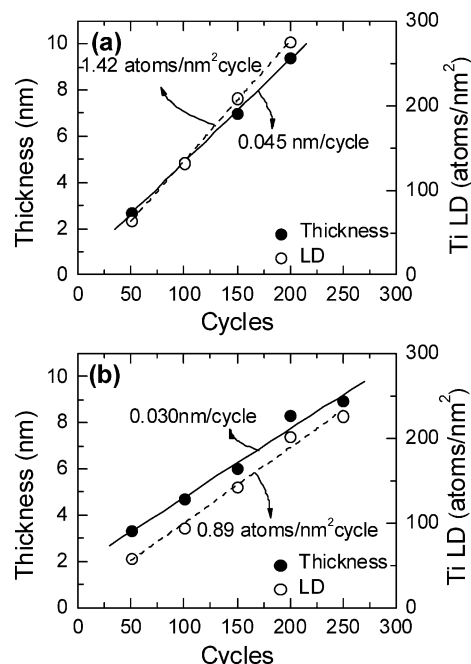


**Figure 1.** Thickness (solid symbols) and layer density (open symbols) of the TiO<sub>2</sub> films grown on a Ru substrate using (a) H<sub>2</sub>O and (b) O<sub>3</sub> as the oxygen sources as a function of  $n_{cy}$ .

## III. Results and Discussion

### A. Growth of Component Oxide TiO<sub>2</sub> and PbO<sub>x</sub> Films.

The growth of TiO<sub>2</sub> thin films was attempted using two different oxygen sources, H<sub>2</sub>O and O<sub>3</sub>. Figure 1a,b shows the changes in the thickness and the Ti LD of the TiO<sub>2</sub> films grown on a Ru substrate using H<sub>2</sub>O and O<sub>3</sub> as oxygen sources, respectively, as a function of the number of deposition cycles ( $n_{cy}$ ). A single deposition cycle in the ALD of binary oxide films, such as TiO<sub>2</sub> and PbO<sub>x</sub>, consisted of precursor pulse/purging and oxygen source pulse/purging steps. The thickness and Ti LD of the TiO<sub>2</sub> films increased linearly with increasing  $n_{cy}$ . It should be noted that, at this deposition temperature, the GPC of a TiO<sub>2</sub> film using H<sub>2</sub>O (0.045 nm) was 50% higher than that using O<sub>3</sub> (0.030 nm). These growths per cycle are comparable to those reported elsewhere.<sup>15,16</sup> This suggests that H<sub>2</sub>O is more effective for the growth of TiO<sub>2</sub> than O<sub>3</sub> by forming a hydroxyl terminated surface, whatever the reaction mechanism involved in the latter. Moreover, it was recently reported that O<sub>3</sub>, in addition to hydroxyl groups, leads to the formation of mainly formate and carbonate species at the deposition temperature studied, which are expected to be less reactive toward metal complexes.<sup>17,18</sup> In addition, the bulk density of a TiO<sub>2</sub> film using H<sub>2</sub>O was higher than that using O<sub>3</sub>, very probably because of the incomplete removal of more stable ligands, such as formates (see Figure S1 in the Supporting Information).

PbO<sub>x</sub> thin films were also grown using H<sub>2</sub>O and O<sub>3</sub> as oxygen sources. A modified ALD process, described below, was used to reduce the consumption of the Pb precursor in the deposition processes. The increase in the LD of the PbO<sub>x</sub> film was examined every 100 deposition cycles; that is, the samples were unloaded from the ALD chamber every 100 deposition cycles, and the LDs of the Pb were measured by XRF. The samples were loaded into the ALD chamber again for subsequent PbO<sub>x</sub> growth. Furthermore, prior to the ALD of PbO<sub>x</sub> using O<sub>3</sub>, rather thick ( $n_{cy} = 400$ ) PbO<sub>x</sub> films were deposited on the substrates using H<sub>2</sub>O to protect the substrates from being damaged.<sup>19</sup> Figure 2a,b shows the changes in the Pb LD of the PbO<sub>x</sub> films

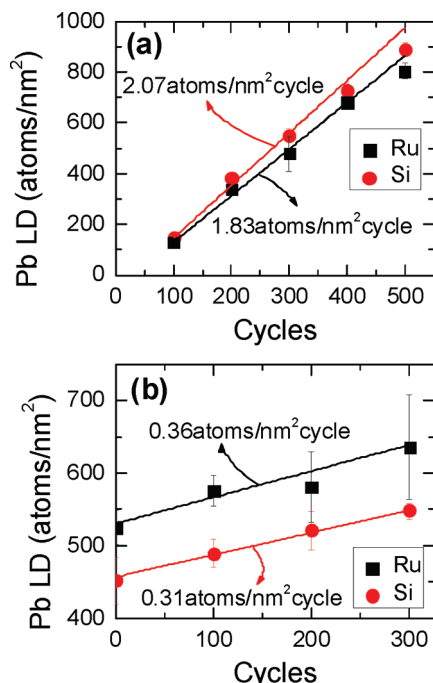


**Figure 2.** Layer density of the  $\text{PbO}_x$  films grown on Ru and Si substrates as a function of  $n_{cy}$  for (a)  $\text{H}_2\text{O}$  and (b)  $\text{O}_3$  oxygen sources. In (b), the Pb LD values at zero growth cycle correspond to the amount of Pb deposited for the  $\text{PbO}_x$  protection layer.

grown on Si and Ru substrates using  $\text{H}_2\text{O}$  and  $\text{O}_3$  as oxygen sources, respectively, as a function of  $n_{cy}$ . In Figure 2b, the y intercept corresponds to the Pb LD of the  $\text{PbO}_x$  layer grown using  $\text{H}_2\text{O}$  as the protection layer. The LD per cycle of the  $\text{PbO}_x$  film grown using  $\text{O}_3$  (0.36 atoms/ $\text{nm}^2$ ·per cycle on Ru and 0.31 atoms/ $\text{nm}^2$ ·per cycle on Si) was much lower than that using  $\text{H}_2\text{O}$  (1.83 atoms/ $\text{nm}^2$ ·per cycle on Ru and 2.07 atoms/ $\text{nm}^2$ ·per cycle on Si). Although rather thick  $\text{PbO}_x$  films from previous depositions had coated the Ru surface, damage to the Ru electrode from  $\text{O}_3$  still occurred with increasing  $n_{cy}$  using  $\text{O}_3$ . The lower GPC of  $\text{PbO}_x$  films grown using  $\text{O}_3$  suggests that the reaction sites generated by  $\text{O}_3$  are less active or have lower densities than those generated by  $\text{H}_2\text{O}$  ( $-\text{OH}$ ). Because  $\text{O}_3$  was less favorable compared to  $\text{H}_2\text{O}$  for  $\text{PbO}_x$  growth,  $\text{O}_3$  was not used as an oxygen source for the Pb precursor in PTO film growth.

**B. Growth of  $\text{PbTiO}_3$  Films.** The growth of PTO thin films was attempted using the two different oxygen sources for the Ti precursor but only  $\text{H}_2\text{O}$  for the Pb precursor. Processes A and B adopted  $\text{H}_2\text{O}$  and  $\text{O}_3$  as the oxygen source for the Ti precursor, respectively (see Figure 3). The LDs and GPCs were measured for both processes (A and B) as a function of Pb/Ti exposure ratio, that is, as a function of the ratio between the number of  $\text{PbO}_x$  and  $\text{TiO}_2$  growth subcycles in a single supercycle (where a supercycle is the repetition unit of a given deposition sequence). (For example, in the cases of Pb/Ti exposure ratios of 1/2, 1/1, and 3/2, the sequences  $\text{PbO}_x$ – $\text{TiO}_2$ – $\text{TiO}_2$ ,  $\text{PbO}_x$ – $\text{TiO}_2$ , and  $\text{PbO}_x$ – $\text{TiO}_2$ – $\text{PbO}_x$ – $\text{TiO}_2$ – $\text{PbO}_x$  were the respective supercycles for these depositions.) The total number of growth cycles ( $n_{\text{tot}}$  = the product of the number of supercycles and the total number of  $\text{PbO}_x$  and  $\text{TiO}_2$  growth cycles in a single supercycle) was controlled to be within 96–100 according to the respective Pb/Ti exposure ratios. Figure 4a,c shows the changes in the Pb/Ti concentration ratio and the sum of the Pb and Ti LDs of PTO thin films for processes A and B, respectively. The overall cation concentra-

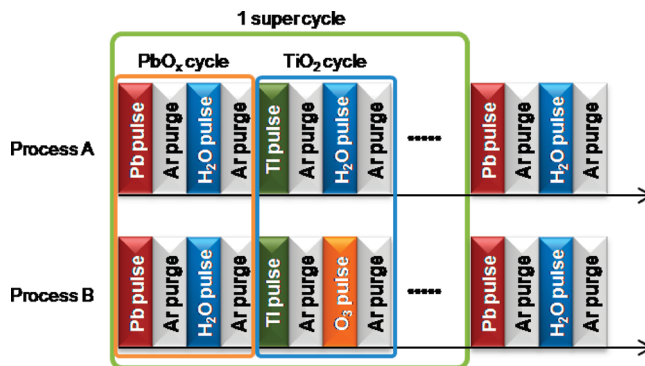


**Figure 3.** Schematic diagram of the deposition sequences of processes A and B.

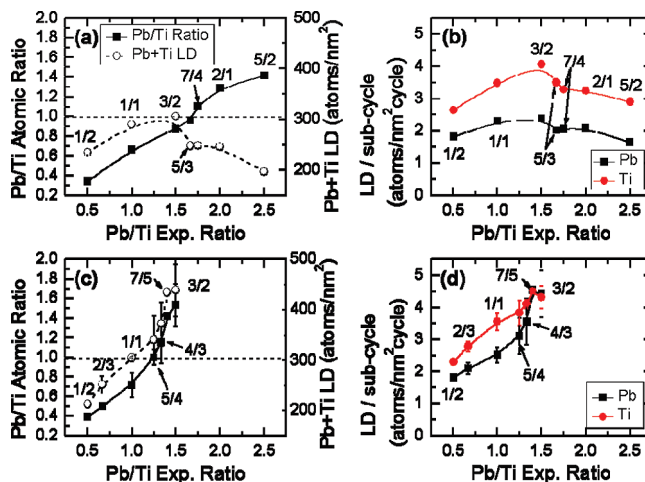


**Figure 4.** Pb/Ti composition ratio (solid symbols), LD (open symbols), and LD per subcycle of Pb and Ti in the PTO films grown using processes (a, b) A and (c, d) B as a function of the Pb/Ti exposure ratio.

tion ratio could be adjusted by controlling the Pb/Ti exposure ratio. Figure 4b,d shows the changes in the LD per Pb and Ti subcycle as a function of the Pb/Ti exposure ratio for processes A and B, respectively. The LD per Pb (or Ti) subcycle was calculated by dividing the total Pb (or Ti) LD by the total number of  $\text{PbO}_x$  (or  $\text{TiO}_2$ ) growth cycles. This corresponds to the number of Pb (or Ti) atoms that are incorporated in the unit area ( $\text{nm}^2$ ) of the PTO film during a single  $\text{PbO}_x$  (or  $\text{TiO}_2$ ) growth cycle. Watanabe et al. calculated the mole area density of a (100) plane of an ideal PTO single crystal (lattice parameter  $\sim 0.4$  nm) to be  $1.0 \times 10^{-9}$  mol/ $\text{cm}^2$ .<sup>5</sup> This mole area density can be converted to the LD for the respective metal atoms of  $\sim 6.2$  atoms/ $\text{nm}^2$ . Therefore, the LD per Pb (or Ti) subcycle in Figure 4b,d shows that the GPC of the films is less than a monolayer. This is believed to be due to steric hindrance of the adsorbing precursor molecules.<sup>20</sup> In process A, the LD of the PTO film reached a maximum when the cation composition of the film was nearly stoichiometric (Pb/Ti concentration ratio  $\sim 1$ ). However, the Pb-deficient or Pb-excess PTO films had a smaller LD, which suggests that the deposition process is most effective under the conditions where a stoichiometric PTO film is grown. In contrast, in process B, the LD of the PTO thin films continued to increase with increasing Pb/Ti exposure ratio, even when the film composition ratio exceeded the stoichiometry. Hence, the maximum experimental Pb/Ti exposure ratio was limited to 1.5, even though it was extended to 2.5 for process A. Figure 4a,c also shows that stoichiometric PTO films



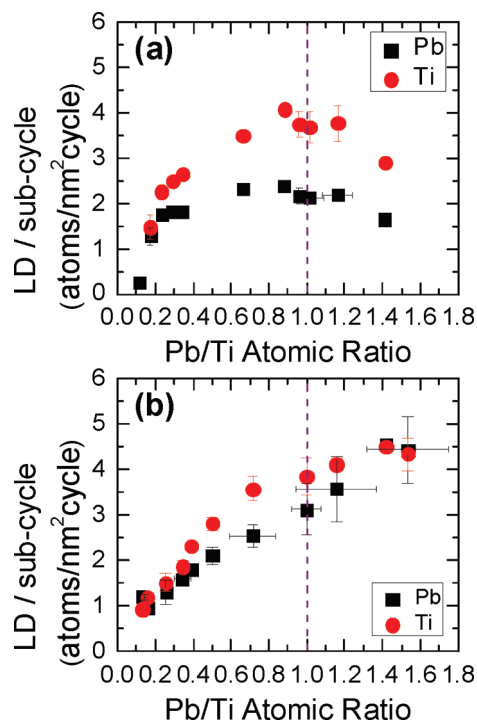


**Figure 5.** Pb and Ti LD per subcycle of PTO films grown on a Ru substrate using processes (a) A and (b) B as a function of the Pb/Ti composition ratio in the PTO films.

can be obtained by process B with a lower Pb/Ti exposure ratio ( $\sim 5/4$ ) than process A (from  $3/2$  to  $7/4$ ).

Figure 5a,b, which presents the changes in the Pb and Ti LD per subcycle as a function of the Pb/Ti concentration ratio in the films grown on the Ru substrate using processes A and B, respectively, shows more clearly the different trends of GPC for both processes. In process A, the Pb and Ti LD per subcycle increased with increasing Pb/Ti concentration ratio in the films, where the ratio is  $< \sim 1$ . It shows a maximum value at a Pb/Ti concentration ratio of  $\sim 1$  and decreases at a Pb/Ti concentration ratio  $> \sim 1$ . In contrast, in process B, the Pb LD per subcycle increased almost linearly with increasing Pb/Ti concentration ratio in the films up to the experimental range adopted in this study (i.e., 1.5). The density of the PTO films grown by process A was slightly higher than that by process B (see the Supporting Information, Figure S2).

The differences between processes A and B were attributed to the different oxygen sources used for the Ti precursor. The highest GPC under the cation stoichiometric condition in process A could be understood from the catalytic and thermodynamic effects of the PTO phase. The adsorption of Pb or Ti is catalyzed by the PTO phase because the PTO phase is more thermodynamically stable than any other binary oxide phases. The standard enthalpy of formation of PTO is  $-1195.7$  kJ/mol at 500 K, which is smaller than the sum of those of the other binary oxide phases (PbO,  $-216.9$  kJ/mol; TiO<sub>2</sub> (anatase),  $-937.4$  kJ/mol; and TiO<sub>2</sub> (rutile),  $-943.6$  kJ/mol at 500 K).<sup>21</sup> Although the as-grown films are an amorphous structure, the local chemical bonding structure might be similar to that of crystalline material. The enthalpy term of free energy is largely determined by the chemical bonding so that this argument may hold even for amorphous film growth. However, the increasing GPC with increasing Pb concentration, even under Pb-excess conditions in process B, requires another model for growth, as will be shown in the next part of this paper. This is somewhat unusual behavior considering that the GPCs of PbO<sub>x</sub> and TiO<sub>2</sub> films using O<sub>3</sub> were lower than those using H<sub>2</sub>O.

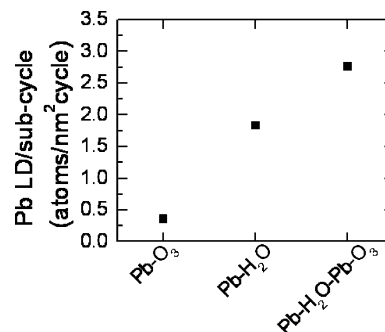


**Figure 6.** Pb LD per cycle of PbO<sub>x</sub> films grown using different PbO<sub>x</sub> deposition sequences.

**C. Growth Mechanism of PTO Films.** In this section, before discussing the growth mechanisms involved in processes A and B, the growth behaviors of PTO and PbO<sub>x</sub> thin films are examined more in detail using a range of deposition sequences, where H<sub>2</sub>O and O<sub>3</sub> oxygen sources were used in different ways. This was expected to be useful in understanding the different growth mechanisms of PTO films according to processes A and B.

First of all, the effect of the oxygen source used to deposit a layer of titania for the subsequent growth of a layer of PbO<sub>x</sub> was considered. This study was already published elsewhere.<sup>19</sup> It shows that (i) a PbO<sub>x</sub> layer enhances the growth of the TiO<sub>2</sub> layer, and vice versa (this has been attributed to a catalytic effect, such as those already observed in a multioxide ALD component<sup>4,5,22</sup>), (ii) the growth of PbO<sub>x</sub> on TiO<sub>2</sub> is enhanced when H<sub>2</sub>O was used as an oxygen source for the Ti precursor compared with O<sub>3</sub>, and (iii) the Pb/Ti ratio increases more quickly when O<sub>3</sub> is used to grow the TiO<sub>2</sub> layer. This last point is understandable because, according to the GPC of titania using O<sub>3</sub>, a thinner TiO<sub>2</sub> layer is deposited in this case, finally leading to a higher Pb/Ti ratio. From this study, no mechanism explaining the difference in growth according to the oxygen sources can be proposed. As a matter of fact, the same growth behavior in the case of the pure oxides (i.e., TiO<sub>2</sub> and PbO<sub>x</sub>) is observed; that is, the GPC is lower when ozone is used.

Second, the alternating use of H<sub>2</sub>O and O<sub>3</sub> in the same sequence for the growth of pure PbO<sub>x</sub> was examined. Figure 6 shows the Pb LD per cycle of the PbO<sub>x</sub> films grown using Pb-O<sub>3</sub>, Pb-H<sub>2</sub>O, and Pb-H<sub>2</sub>O-Pb-O<sub>3</sub> as the deposition sequences. In the Pb-O<sub>3</sub> and Pb-H<sub>2</sub>O-Pb-O<sub>3</sub> sequences, a PbO<sub>x</sub> film ( $n_{cy} = 400$  and  $100$ , respectively) was deposited on the Ru substrate using H<sub>2</sub>O before the ALD of PbO<sub>x</sub> using O<sub>3</sub> in order to protect the electrodes from being damaged by O<sub>3</sub>, as mentioned previously. The samples with the protecting PbO<sub>x</sub> layer were unloaded from the ALD chamber to measure the Pb LD and then used for the subsequent deposition of PbO<sub>x</sub> films. The samples were also unloaded from the ALD chamber after the ALD process using the respective deposition sequences for 100 cycles to measure the Pb LD and reloaded into the ALD chamber for the subsequent 100 ALD cycles. The Pb LDs per cycle shown in Figure 6 were estimated from the slope of the line of best fit of the Pb LD versus number of cycle data. As mentioned in the previous part, the GPC of PbO<sub>x</sub> films deposited using the Pb-H<sub>2</sub>O sequence was much higher than that using the Pb-O<sub>3</sub> sequence.

An interesting finding is that the GPC of the Pb-H<sub>2</sub>O-Pb-O<sub>3</sub> sequence was surprisingly higher than that of the Pb-H<sub>2</sub>O sequence, even though the Pb-O<sub>3</sub> sequence has a much lower GPC. Note that the Pb LD per cycle for the Pb-H<sub>2</sub>O-Pb-O<sub>3</sub> sequence was determined by considering the two injections of the Pb precursor in a supercycle.

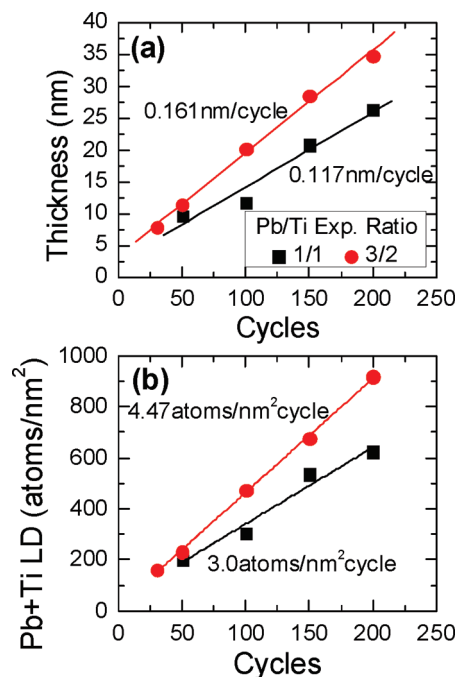


**Figure 7.** Variations in the (a) thickness and (b) layer density of the PTO films grown by process B at Pb/Ti exposure ratios of 1/1 and 3/2, respectively, as a function of  $n_{\text{tot}}$ . The GPC of the PTO films at a Pb/Ti exposure ratio of 3/2 was higher than that at 1/1.

Finally, to gain more information on process B, PTO film growth with different Pb/Ti exposure ratios was examined more closely. Figure 7a,b shows the changes in the thickness and LD of PTO films grown by process B at Pb/Ti exposure ratios of 1/1 and 3/2, respectively, as a function of  $n_{\text{tot}}$ . The deposition sequences of each process with the respective Pb/Ti exposure ratio are as follows:

Pb/Ti = 1/1: [Pb–H<sub>2</sub>O–Ti–O<sub>3</sub>]–[Pb–H<sub>2</sub>O–Ti–O<sub>3</sub>]–[Pb–H<sub>2</sub>O–Ti–O<sub>3</sub>]–...

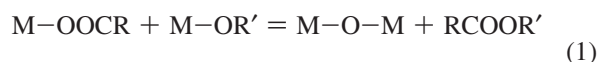
Pb/Ti = 3/2: [Pb–H<sub>2</sub>O–Ti–O<sub>3</sub>–Pb–H<sub>2</sub>O–Ti–O<sub>3</sub>–Pb–H<sub>2</sub>O]–[Pb–H<sub>2</sub>O–...

Here, the square bracket corresponds to a supercycle. In the case of 1/1, all Pb steps except for the very first step always followed the previous O<sub>3</sub> step (indicated by the underline), which was used to grow the TiO<sub>2</sub> layer. On the other hand, in the case of 3/2, the first Pb step of each supercycle followed the H<sub>2</sub>O step (indicated by the wavy underline), whereas other Pb steps followed the O<sub>3</sub> step with the exception of the very first step. The GPC for the 3/2 process was higher than that of the 1/1 process (Figures 4b and 7). Although the Ti–O<sub>3</sub>–Pb–H<sub>2</sub>O sequence (process B) resulted in a higher PbO<sub>x</sub> incorporation than the Ti–H<sub>2</sub>O–Pb–H<sub>2</sub>O sequence (process A), the formation of –OH groups on the surface by H<sub>2</sub>O at the first Pb step of each supercycle using the 3/2 exposure ratio also contributes to the enhanced adsorption of Pb precursor molecules.

In the ALD of metal oxides using H<sub>2</sub>O as an oxygen source, the film grows via a reaction between the supplied precursor molecules and hydroxyl-terminated surface groups. For instance, it is expected that, in process A, the injected Pb(dmamp)<sub>2</sub> precursor molecules absorb onto the –OH surface sites by producing an alcohol (dmampH) as a reaction byproduct. During the subsequent H<sub>2</sub>O pulse step, another dmamp ligand of the chemisorbed Pb precursor molecules is also liberated by generating dmampH again.<sup>23</sup> During the ALD of metal oxides using O<sub>3</sub> as the oxygen source, it was recently reported that O<sub>3</sub>

exposure leads to formate, carbonate, and hydroxyl groups on the surface.<sup>17,18,24</sup> According to Goldstein et al., a large amount of formate surface species was formed by a reaction between trimethylaluminum (TMA) and O<sub>3</sub>.<sup>17</sup> A small quantity of carbonate and hydroxyl species was also formed with their quantity becoming significant only at temperatures higher than 550 K. However, ALD using TMA and H<sub>2</sub>O generated only hydroxyl species without formate or carbonate groups.<sup>17</sup>

In this study, the deposition of PbO<sub>x</sub> and PTO is expected to lead to similar surface species when O<sub>3</sub> was used as an oxygen source. The higher Pb incorporation rate in process B suggests that a reaction between the dmamp ligands of the Pb precursor molecules and formate or carbonate groups occurs and results in the enhanced absorption of Pb precursor molecules as compared with process A during the Pb precursor pulse step following the O<sub>3</sub> pulse. It is unlikely that this reaction is related to the amine group of the dmamp ligand as it is a tertiary amine. A possible reaction between surface formates and alkoxides is a direct condensation, called ester elimination, similar to acid-catalyzed transesterification where the electropositive metal center acts as a Lewis acid.<sup>25</sup> As a matter of fact, it was recently reported that the reaction of metal alkoxides and carboxylic acids (acetic and formic acid) can be applied to ALD for the deposition of conformal oxide films.<sup>26,27</sup> In this case, the oxide formation takes place via an ester elimination condensation step between carboxylic and alkoxy ligands without the formation of intermediate –OH groups (cf. eq 1). This work proved that surface carboxylates can be efficiently removed by the reaction with metal alkoxides, even at low temperatures. It should be pointed out that the reaction mechanism leading to the removal of the surface formate groups generated by the O<sub>3</sub> pulse could be similar to the one reported in the ALD of metal alkoxides and carboxylic acids.



Moreover, the synthesis of PTO by sol–gel processes (i.e., in solution) using a large variety of precursors (alkoxide, acetate, oxide, and acetic acid modified alkoxide) has been thoroughly studied.<sup>28,29</sup> The reaction of these precursors at a moderate temperature often leads to oxo complexes that are finally hydrolyzed in order to obtain the oxide. This is what happens when Ti(O<sup>i</sup>Pr)<sub>4</sub> and lead(II) acetate [Pb(OAc)<sub>2</sub>] are reacted in hexane at room temperature.<sup>28</sup>

In the system studied here, these complexes can be formed at the surface of the Ti oxide due to the reaction of Pb(dmamp)<sub>2</sub> with surface formate species. During the subsequent H<sub>2</sub>O step, the hydrolysis of these surface complexes leads to the formation of M–O–M bonds and the complete removal of the ligands.

It is not easy to determine which reaction mechanism is more likely responsible for the formation of PTO by process B. From the different experiments reported above, it is clear that the use of O<sub>3</sub> for TiO<sub>2</sub> deposition slightly slows down the growth of Ti oxide, although a thicker PbO<sub>x</sub> layer can be deposited compared to the process using H<sub>2</sub>O only.

On the other hand, the fact that the succession of different oxygen sources increases the growth per cycle suggests that the formation of molecular complexes by the reaction between surface formate species and Pb(dmamp)<sub>2</sub> is the most likely mechanism as the formation of oxo clusters can very probably form independently of the stoichiometry of the deposited film. As a matter of fact, this would explain the fact that the Pb/Ti atomic ratio of the film can be increased continuously with the

Pb/Ti exposure ratio, on the one hand, and the need of water for removing the ligands left and for inducing the condensation of the molecular complexes, on the other hand. Furthermore, the higher PbO<sub>x</sub> incorporation also increases the growth of the next TiO<sub>2</sub> layer. Therefore, the continuously increasing tendency of the overall GPC for process B shown in Figures 4 and 5 can be understood from these models.

#### IV. Conclusions

PTO thin films were grown on Si and Ru substrates by thermal ALD at 200 °C using H<sub>2</sub>O and O<sub>3</sub> as the oxygen sources. The roles of the oxygen sources on the ALD behavior of each component oxide, TiO<sub>2</sub> and PbO<sub>x</sub>, and the PTO films, as well as the influence of the cation composition of the growing surface on the growth behavior, were examined. Film growth was most effective under the appropriate Pb/Ti exposure ratio for achieving a stoichiometric Pb/Ti ratio (=1) when H<sub>2</sub>O was used as the oxygen source for both Pb and Ti precursors due to the catalytic and thermodynamic effect of the PTO phase. On the other hand, the GPC increased with increasing Pb/Ti exposure ratio when H<sub>2</sub>O and O<sub>3</sub> were used as the oxygen sources for the Pb and Ti precursors, respectively.

The growth mechanisms of the PbO<sub>x</sub> films grown using various deposition sequences and oxygen sources were also investigated. H<sub>2</sub>O was much more efficient than O<sub>3</sub> for PbO<sub>x</sub> ALD. However, a proper combination of oxygen source exposure sequences could increase the growth per cycle to a higher value than that achieved with the H<sub>2</sub>O only process. This was attributed to a reaction mechanism involving the direct condensation between surface formate species and alkoxy species. Moreover, it was found that the Ti–O<sub>3</sub>–Pb–H<sub>2</sub>O sequence resulted in a higher growth per cycle for the PbO<sub>x</sub> layer than the Ti–H<sub>2</sub>O–Pb–H<sub>2</sub>O sequence. The higher rate of PbO<sub>x</sub> incorporation also increases the growth per cycle of the TiO<sub>2</sub> layer. Finally, the growth per cycle of the PTO film increased even when the film composition became Pb-rich in the ALD process using O<sub>3</sub> to deposit the TiO<sub>2</sub> layer.

**Acknowledgment.** The study was supported by the Converging Research Center Program through the National Research Foundation of Korea (NRF) funded by the Ministry of Education, Science and Technology (2009-0081961), the National Program for 0.1 Terabit NVM Devices of the Korean Government, the World Class University program through the National Research Foundation of Korea funded by the Ministry of Education, Science and Technology (R31-2008-000-10075-0) and (R31-10013), and FCT Project No. PTDC/CTM/65667/2006.

**Supporting Information Available:** The Supporting Information contains two graphs on the changes in the bulk density

of a TiO<sub>2</sub> film as a function of the number of ALD cycles (Figure S1), the variations in the bulk density of a PTO film as a function of the Pb/Ti composition ratio in the PTO film (Figure S2), and one graph on the AES depth profiles of the PbO<sub>x</sub> films using different oxygen sources (Figure S3). This material is available free of charge via the Internet at <http://pubs.acs.org>.

#### References and Notes

- (1) Suntola, T. *Mater. Sci. Rep.* **1989**, *4*, 261.
- (2) Scott, J. F. *Ferroelectric Memories*; Springer: Heidelberg, Germany, 2000.
- (3) Harjuoja, J.; Kosola, A.; Putkonen, M.; Niinisto, L. *Thin Solid Films* **2006**, *496*, 346.
- (4) Hwang, G. W.; Lee, H. J.; Lee, K.; Hwang, C. S. *J. Electrochem. Soc.* **2007**, *154*, G69.
- (5) Watanabe, T.; Hoffmann-Eifert, S.; Mi, S.; Jia, C.; Waser, R.; Hwang, C. S. *J. Appl. Phys.* **2007**, *101*, 014114.
- (6) Watanabe, T.; Hoffmann-Eifert, S.; Peter, F.; Mi, S.; Jia, C.; Hwang, C. S.; Waser, R. *J. Electrochem. Soc.* **2007**, *154*, G262.
- (7) Watanabe, T.; Hoffmann-Eifert, S.; Hwang, C. S.; Waser, R. *J. Electrochem. Soc.* **2007**, *155*, D715.
- (8) Cho, M.; Jeong, D. S.; Park, J.; Park, H. B.; Lee, S. W.; Park, T. J.; Hwang, C. S. *Appl. Phys. Lett.* **2004**, *85*, 5953.
- (9) Cho, M.; Park, H. B.; Park, J.; Lee, S. W.; Hwang, C. S.; Jeong, J.; Kang, H. S.; Kim, Y. W. *J. Electrochem. Soc.* **2005**, *152*, F49.
- (10) Rahtu, A.; Alaranta, T.; Ritala, M. *Langmuir* **2001**, *17*, 6506.
- (11) Kang, S. Y.; Hwang, C. S.; Kim, H. J. *J. Electrochem. Soc.* **2005**, *152*, C15.
- (12) Kawano, K.; Nagai, A.; Kosuge, H.; Shibutani, T.; Oshima, N.; Funakubo, H. *Electrochem. Solid-State Lett.* **2006**, *9*, C107.
- (13) Kim, S. K.; Lee, S. Y.; Lee, S. W.; Hwang, G. W.; Hwang, C. S.; Lee, J. W.; Jeong, J. *J. Electrochem. Soc.* **2007**, *154*, D95.
- (14) Han, J. H.; Lee, S. W.; Choi, G.-J.; Lee, S. Y.; Hwang, C. S.; Dussarrat, C.; Gatineau, J. *Chem. Mater.* **2009**, *21*, 207.
- (15) Kim, W. D.; Hwang, W. D.; Kwon, O. S.; Kim, S. K.; Cho, M.; Jeong, D. S.; Lee, S. W.; Seo, M. H.; Hwang, C. S.; Min, Y. S.; Cho, Y. J. *J. Electrochem. Soc.* **2005**, *152*, C552.
- (16) Kim, S. K.; Lee, S. Y.; Seo, M.; Choi, G.-J.; Hwang, C. S. *J. Appl. Phys.* **2007**, *102*, 024109.
- (17) Goldstein, D. N.; McCormick, J. A.; George, S. M. *J. Phys. Chem. C* **2008**, *112*, 19530.
- (18) Rai, V. R.; Agarwal, S. *J. Phys. Chem. C* **2008**, *112*, 9552.
- (19) Lee, H. J.; Park, M. H.; Hwang, C. S. *ECS Trans.* **2009**, *19*, 829.
- (20) Puurunen, R. L. *J. Appl. Phys.* **2005**, *97*, 121301.
- (21) Barin, I. *Thermochemical Data of Pure Substances*; VCH: Weinheim, Germany, 1989.
- (22) Kwon, O. S.; Lee, S. W.; Han, J. H.; Hwang, C. S. *J. Electrochem. Soc.* **2007**, *154*, G127.
- (23) Yang, T. S.; Cho, W.; Kim, M.; Ahn, K.-S.; Chung, T.-M.; Kim, C. G.; Kim, Y. *J. Vac. Sci. Technol., A* **2005**, *23*, 1238.
- (24) Kwon, J.; Dai, M.; Halls, M. D.; Chabal, Y. J. *Chem. Mater.* **2008**, *20*, 3248.
- (25) Caruso, J.; Hampden-Smith, M. J. *J. Sol-Gel Sci. Technol.* **1997**, *8*, 35.
- (26) Rauwel, E.; Clavel, G.; Willinger, M.-G.; Rauwel, P.; Pinna, N. *Angew. Chem., Int. Ed.* **2008**, *47*, 3592.
- (27) Clavel, G.; Rauwel, E.; Willinger, M.-G.; Pinna, N. *J. Mater. Chem.* **2009**, *19*, 454.
- (28) Hubert-Pfalzgraf, L. G.; Daniele, S.; Papiernik, R.; Massiani, M.-C.; Septe, B.; Vaissermann, J.; Daran, J.-C. *J. Mater. Chem.* **1997**, *7*, 753.
- (29) Schwartz, R. W. *Chem. Mater.* **1997**, *9*, 2325.

JP101423F